

On the AoI-Aware Status Update in Buffer-aided Wireless Powered Internet of Things Network

Tianheng Wang, Shuo Wang, Xiaolong Lan, *Member, IEEE*, Yong Liu, *Member, IEEE*,
Qingchun Chen, *Senior Member, IEEE*, Pei Xiao, *Senior Member, IEEE*

Abstract—In this paper, we focus on buffer-aided wireless powered Internet of Things (IoTs) comprising of one wireless access point (AP) and multiple devices, where the AP provides energy to all devices via downlink radio frequency (RF) energy beams. All devices utilize the harvested energy to transmit their data to the AP in a time-division multiple access (TDMA) manner. Every device is assumed to be provisioned with energy storage and data buffer to store the collected energy from the AP and its data, respectively. The problem of minimizing the long-term average age of information (AoI) of the system is formulated in this paper. By solving the problem under the Lyapunov optimization framework, the AoI-aware adaptive transmission scheme is obtained, in which downlink RF energy beamforming, downlink energy transfer and uplink access, as well as transmit power and transmission rate by every device, will be jointly adjusted in order to minimize average weighted AoI according to the underlying channel state information (CSI), the buffer state information (BSI), the energy-consumption status information (ESI) of all terminals, as well as the AoI status information (ASI). Our analysis unveils that, the status update rate at devices has a significant impact on the achievable AoI performance, and the minimum average weighted AoI can only be realized at a reasonable status update rate, which is neither too high nor too low. Moreover, flexible AoI-aware scheme can be realized by adjusting either the AoI priority level or the AoI weighting coefficient.

Index Terms—AoI-Aware Mechanism; Wireless Powered Internet of Things; Random Status Update.

I. INTRODUCTION

The work of Tianheng Wang, Shuo Wang and Qingchun Chen was supported by the Lingnan Yingjie Project by Guangzhou Municipal Government, and the Key Discipline Project of Guangzhou Education Bureau under Grant No. 202255467. The work of Xiaolong Lan was supported in part by the Natural Science Foundation of China under grant No. 62101358, China Postdoctoral Science Foundation under grant No.2020M683345, Joint Innovation Fund of Sichuan University and Nuclear Power Institute of China under grant No. HG2022143, and Sichuan University-Dazhou People's Government Strategic Cooperation Special Fund Project under grant No.2022CDDZ-10. The work of Yong Liu was supported in part by the National Natural Science Foundation of China under grant No. 61901180, Natural Science Foundation of Guangdong Province under grant No. 2022A1515010111 and 2023A1515012890, and Science Technology Project of Guangzhou under grant No. 202201010574. (*Corresponding author: Qingchun Chen.*)

T. Wang, S. Wang, and Q. Chen are with the School of Electronics and Communication Engineering, Guangzhou University, Guangzhou, 510006, China (e-mail: qxj123721@163.com, 2112019049@e.gzhu.edu.cn, qcchen@gzhu.edu.cn). X. Lan is with the School of Cyber Science and Engineering, Sichuan University, Chengdu 610065, China (e-mail: xiaolonglan1112@gmail.com). Y. Liu is with the School of Electronics and Information Engineering, South China Normal University, Foshan, 528225, China (e-mail: yliu@m.scnu.edu.cn). P. Xiao is with Institute for Communication Systems (ICS), Home for 5GIC 6GIC, University of Surrey, Guildford, Surrey, GU2 7XH, United Kingdom. (e-mail: p.xiao@surrey.ac.uk).

MORE and more Internet of Things (IoT) devices are widely deployed to enable smart transportation, home, and medical applications [1]- [3]. The ultra-reliable low latency communications (URLLC) in 5G networks serve as an enabler for meeting the emerging latency-sensitive service requirements. However, it should be noted that traditional communication delay metrics, such as network delay and its jitter, can not characterize and capture the data freshness requirements of the increasing IoT applications. In recent years, the concept of age of information (AoI) has received a lot of attention to measure the freshness of the received data from the receiver perspective [4], [5]. AoI captures the elapsed time between the present time and the generation time of the latest data packet at source, which allows us to effectively measure the information timeliness of the received data packets at the destination [6]- [9].

A. Related Works

Ever since its inception in the literature, the concept of AoI has been widely used to assess delay-sensitive communication services [10]- [25]. The minimum realized AoI problem for single-link state monitoring system and multi-link state monitoring system were studied in [13]- [16] for the given Bernoulli data generation model (i.e., packets are generated within each time slot independently with probability λ). The long-term average weighted AoI performance of a system with one single base station serving multiple users with different service flows under given arrival constraints were studied in [17]- [19], in which three queuing rules of *first-come, first-served* (FCFS), *last-come, first-served* (LCFS), and *no-queue* were considered, and it was shown that the optimal stationary randomized policy and the max-weight policy were recommended to enhance the achievable AoI performance. In addition, it was unveiled that, by performing Lyapunov optimization [47], the maximum-weight policy was capable of approaching the system long-term average weighted AoI lower bound.

The AoI-aware scheduling problem in an uplink multiple access IoT system was studied in [20], and two multiple access scheduling algorithms of cyclic scheduling detection (CSD) and fictitious polynomial mapping (FPM) were proposed to guarantee the maximum AoI threshold requirements by all users for small-scale network and large-scale network, respectively. An age-independent stationary randomized policy (AI-SRP) for the unlink data updates in a TDMA based multiple access network was studied in [21] to minimize the

long-term weighted average AoI. The information freshness of single-server multi-source queueing models under the *FCFS* serving policy was studied in [22]. The exact average AoI for the case with exponentially distributed service time (i.e., a multi-source $M/M/1$ queueing model) was derived to obtain approximate average AoI for multi-source $M/G/1$ queueing model with general service time distribution. An AoI-aware transmission scheme was studied in [23] to reduce AoI in NOMA-based downlink systems. An age-optimal heterogeneous traffic scheduling scheme was considered in [24] to improve the information freshness of status update traffic while satisfying timely throughput constraints. In [25], the resource allocation problem in an energy harvesting wireless sensor networks (EH-WSNs) using TDMA and frequency-division multiple access (FDMA) was studied to minimize the average AoI, and it was shown that the choice of two multiple access techniques depends on many factors such as the available energy, the number of users, the packet size, and the type of packet sampling (parallel sampling or distributed sampling). Although there have been a plethora of research efforts devoted to different scenarios where AoI is minimized, most of the existing studies assume users with either throughput performance requirements or AoI performance requirements. In practical IoT applications, such as real-time vehicle travel path detection and remote surgery, the system design is expected to reduce AoI as much as possible when meeting certain throughput requirements. This is in fact the first motivation of our work in this paper.

Wireless energy transfer (WET) technology provides a promising energy supply alternative to overcome the energy sustainability issue in the IoT design. In recent years, wireless powered communication networks (WPCN) had received much attention due to its flexibility of using WET and wireless information transmission (WIT) [26]- [32], [37]- [40]. Although RF-based WET techniques can transmit energy from a few meters to several kilometers, the RF signal decays sharply with the increase of transmission distance, which gives rise to lower energy transmission efficiency [30]. Wireless energy beamforming (BF) can be utilized to compensate this drawback by concentrating the RF signal in a specific direction. In [31], the optimal energy beamforming design was proposed to maximize the energy transmission efficiency in a MIMO system. A MISO WPCN was studied in [32] to devise downlink RF-base WET beams such that multiple nodes can use the collected energy to transmit their data in TDMA systems, then the time slot allocation and energy beamforming design were jointly optimized to maximize the overall system throughput performance.

Large of existing research has demonstrated the great potential of introducing data buffer-aided or energy storage into wireless communication system to improve system transmission throughput performance or reduce transmission power overhead [33]- [40]. Data buffer-aided scheme was introduced in [33]- [36] to improve transmission throughput performance of wireless relay networks. It was shown in [37]- [40] that, the use of energy storage in WPCN can efficiently utilize channel state information (CSI) to enhance transmission throughput. When a common power station (PS) is deployed

to provide energy supply to multiple terminals through RF-based energy harvesting techniques such that these terminals can independently transmit their data to the corresponding receivers, it was shown in [38] that, if a certain transmission delay can be tolerated, multiple energy-constrained wireless powered terminals can be effectively supported with less power consumption at the desired data rate. An online buffer-energy-aware adaptive transmission scheme was proposed for wireless powered buffer aided relay communication in [39] to adjust the transmission according to the dynamic CSI, the data buffer state information (BSI), and the energy state information (ESI) for the sake of maximizing the achievable throughput. In [40], the access point (AP) of a wireless network was utilized to provide energy supply via WET to multiple terminals in the downlink, and all terminals then use the harvested energy to transmit their data to the AP in a TDMA manner. A buffer-aided adaptive transmission scheme was proposed to maximize the long-term weighted sum-rate through energy BF design, power allocations, rate control, time allocations, and transmission mode selection subject to average transmit power, peak transmit power, data loss ratio requirements, limited data buffer size as well as energy storage constraint. In addition, the weighted max-min scheduling scheme was proposed to guarantee the fair access requirement by multiple terminals. The works in [39] and [40] disclosed the compromise and inherent tradeoff relationship between the realized system average transmission rate and the incurred time delay. A large number of existing studies have confirmed the great potential of introducing buffer-aided mechanisms in wireless energy harvesting communication systems to improve the system performance. However, there is a paucity of research efforts reported in the literature to explore the realized AoI performance in buffer-aided wireless powered IoT network, which is the second motivation of our work in this paper.

Recently, real-time monitoring system was studied in [41] and [42], in which multiple source nodes are supposed to send update packets to a common destination node in order to maintain the freshness of information at the destination in terms of the average weighted AoI, and all source nodes are powered through wireless energy transfer (WET) by the destination. The long-term average weighted sum of AoI minimization problem was formulated as a Markov decision process (MDP) with finite state and action spaces. Due to the extreme curse of dimensionality in the state space of the formulated MDP, deep reinforcement learning (DRL) algorithm and *Deep Q Network* (DQN) algorithm were proposed in [41] and [42] to learn the age-optimal policy in a computationally-efficient manner. However, only the *generate-at-will* data generation model was considered, which can not completely characterize the effect of the stochastic arrival of data by source nodes on the achieved average weighted AoI performance. In addition, due to the complexity, deep learning approach was employed in [41] and [42] to obtain the age-optimal policy, which is not so obvious to highlight the critical factors that dominate the realized average weighted AoI performance. And this is precisely our third motivation to consider more general task-related status update rates and to derive AoI-aware status update by using a Lyapunov optimization framework in buffer-

aided wireless powered IoT network.

B. The Primary Work and Contributions of This Paper

This paper focuses on an AoI-aware buffer-aided wireless powered IoT network, in which one AP provides energy to multiple devices via downlink RF energy beamforming, and multiple devices utilize the harvested energy to transmit their task-related status update data to AP in a TDMA manner. Every device is assumed to be provisioned with energy storage and data buffer to store the collected energy from the AP and its own task-related status update data, respectively. In order to gain insights into the achievable AoI region and the primary factors that dominate the achievable AoI performance, the problem of minimizing the long-term average weighted AoI of the system is formulated and studied. By solving the problem under the Lyapunov optimization framework, we derive the AoI-aware adaptive transmission scheme to effectively reduce the long-term average weighted AoI of the system, in which the downlink RF energy beamforming, the downlink energy transfer and uplink multiple devices data transmission, as well as the transmit power and transmission rate by every terminal, will be jointly adjusted according to the underlying CSI, the BSI and the ESI, as well as the ASI of different devices on the AP side. The primary work and main contributions of the paper can be summarized as follows:

- Firstly, considering the device task-related randomly generated status update data, we propose an adaptive AoI-aware status update scheme for buffer-aided wireless powered IoT network to reveal the achievable average AoI performance. Our analysis in this paper unveils the fact that, status update rate has a direct impact on the achievable average AoI performance. It is disclosed that there exists an optimal status update rate in terms of the minimum realized long-term average AoI.
- Secondly, our analysis unveils that, given the status update rate, the AoI priority level and the AoI weighting coefficient can be set to adjust the realized average AoI of specific device and the average weighted AoI of system, respectively. Hence, the AoI priority level and the AoI weighting coefficient provide us two methods to flexibly fulfill the status update requirements by specific device and the whole system.

Our analysis in the paper sheds light on how to design an AoI-aware adaptive buffer-aided wireless powered IoT network. The remainder of this paper is organized as follows: in Section II, we present the model of buffer-aided wireless powered IoT network and the average weighted AoI minimization problem formulation. The Lyapunov optimization framework is utilized in Section III to solve the average weighted AoI minimization problem to derive the AoI-aware adaptive status update scheme. The numerical analysis results are presented in Section IV to validate our analysis. Finally, we conclude our work in Section V.

Throughout the paper, bold letters will be used to denote vectors (lowercase) or matrices (uppercase). $(\cdot)^T$ and $(\cdot)^H$ stands for transpose and conjugate transpose, respectively. $|\cdot|$ denotes absolute value and $\|\cdot\|$ denotes Euclidean norm. $tr(\cdot)$

denotes the trace of a matrix, and $\cdot \succeq$ implies that the matrix is semi-definite. $diag(\cdot)$ stands for the diagonalization matrix of a vector.

II. SYSTEM MODEL AND PROBLEM FORMULATION

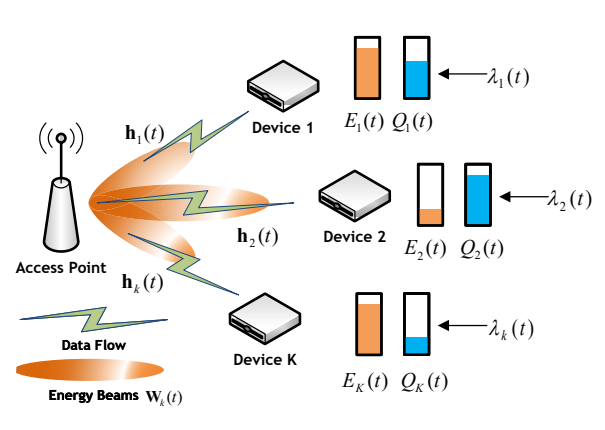


Fig. 1. Buffer-aided Wireless Powered IoT Network.

As shown in Fig. 1, the wireless powered IoT network under study consists of an access point (AP) and K devices, where the AP is assumed to be equipped with N antennas and each device is equipped with a single antenna. All devices are assumed to be energy-constrained nodes that can only harvest energy from the AP through wireless energy harvesting techniques, i.e., the AP transmits energy beams to all devices in the downlink transmission phase, and all devices use the collected energy to transmit their task-related status update data to the AP in the uplink phase. Moreover, all devices are assumed to transmit their independent status update packet to the AP in a TDMA manner. In order to fully explore the potential of data buffer and energy storage to improve the status update performance, we assume that each device has a data buffer and an energy storage to store status update packets (either upper layer task specified status update or sensing data) and the collected energy via wireless energy harvesting, respectively. We consider a time-slot based communication system with T slots, and let $\mathcal{T} = \{0, 1, \dots, T-1\}$ denote the set of time slots. Let $E_k(t)$ and $Q_k(t)$ represent the energy storage state and data buffer state of device k within time slot $t \in \mathcal{T}$, respectively. In each time slot, we assume that the generation of a fresh packet for each device obeys the Bernoulli process with parameter $\lambda(t)$. Let $a_k(t)$ denote the number of fresh packets generated by device k , thus $\mathbb{E}[a_k(t)] = \lambda$ (packets/slot). We use L_k to represent the size of each packet generated by device k (unit: bits). When a fresh packet associated with device k is generated, it will be first buffered in the corresponding data buffer¹, then waits to be scheduled for transmission under the *FCFS* queuing policy.

Let $\mathbf{h}_k(t) \in \mathbb{C}^{N \times 1}$ denote channel coefficients of the link from device k to AP. We assume that all involved wireless channels are block fading, i.e., the channel coefficient is a

¹Since data buffer is assumed, we do not assume packet loss, which might be important in some IoT applications, wherein not only the data freshness, but also the in-order and complete packet delivery are needed.

constant within each time slot, but can vary independently from one slot to the next. We use $K + 1$ binary variables $d_k(t) \in \{0, 1\}$ to indicate whether the downlink energy transfer or uplink data transmission by a specific device k is selected for transmission status update to the AP. More specifically, $d_0(t) = 1$ indicates that the downlink energy transfer mode is selected, otherwise $d_0(t) = 0$. $d_k(t) = 1$ ($k \in \{1, 2, \dots, K\}$) represents that device k is scheduled to transmit its status update to the AP, otherwise $d_k(t) = 0$. Since we assume that the whole system operates in the half-duplex mode, i.e., the energy transfer and data transmission cannot be performed simultaneously, thus the TDM uplink constraint can be given by:

$$\sum_{k=1}^K d_k(t) = 1, \quad \forall t. \quad (1)$$

In this work, we perform centralized scheduling and assume that the AP can obtain perfect channel state information (CSI) by inserting appropriate channel estimation pilots when devices upload their data. In addition, we assume that all devices can feed back their energy storage states and data buffer states (backlogs) to the AP via a dedicated signaling channel. Once the AP obtains the AoI status information (ASI), energy storage state information (ESI), data buffer state information (BSI), and CSIs of all devices, it can adaptively make a transmission control decision accordingly, and informs all devices how to adapt their transmissions. In realistic scenarios, the AP cannot obtain perfect CSIs, and the impact of imperfect CSIs on the AoI-aware buffer-aided wireless powered IoT network will be left for our future work. The symbol notation used in this paper can be summarized in Table 1.

A. Downlink RF Energy Transfer Mode

In time slot t , if $d_0(t) = 1$, the system will operate in the downlink RF energy transmission mode. The AP will transmit energy beams to all devices, such that every device can harvest energy from the received RF signal. The energy transmission beamforming vector of the AP in time slot t is given by:

$$\mathbf{w}(t) = (w_1(t), w_2(t), \dots, w_N(t))^T \in \mathbb{C}^{N \times 1} \quad (2)$$

The transmit power of the AP is given by $P_{AP} = \|\mathbf{w}(t)\|^2 = \text{tr}(\mathbf{w}(t)\mathbf{w}(t)^H)$. The energy beam signal received by device k can be expressed as:

$$y_k(t) = \mathbf{h}_k(t)^H \mathbf{w}(t) s_p(t) + z_k(t), \quad (3)$$

where $s_p(t)$ stands for the signal intended for WET, and $\|s_p(t)\|^2 = 1$. $z_k(t) \sim \mathcal{CN}(0, \sigma^2)$ is the additive white Gaussian noise at device k , respectively. Then the harvested energy by device k is given by

$$\begin{aligned} \mathcal{H}_k(t) &= d_0(t)\eta|\mathbf{h}_k(t)^H \mathbf{w}(t)|^2 \\ &= d_0(t)\eta \text{tr}(\mathbf{h}_k(t)\mathbf{h}_k(t)^H \mathbf{w}(t)\mathbf{w}(t)^H), \end{aligned} \quad (4)$$

where $\eta \in (0, 1)$ is the energy conversion efficiency. For simplicity, here we assume unit duration of each time slot.

B. Uplink Data Transmission Mode

In the t -th time slot, if $d_k(t) = 1$, the system operates in the uplink data transmission mode, and device k will transmit its buffered data packets to the AP by using the harvested energy. The received signal at AP is given by

$$\mathbf{y}_{AP,k}(t) = \sqrt{P_k(t)}\mathbf{h}_k(t)x_k(t) + \mathbf{z}_{AP,k}(t), \quad (5)$$

TABLE I
SYMBOL NOTATION TABLE

Symbol	Definition
K	Total number of devices
N	The number of antennas used for RF energy transfer
θ_k	AoI demand priority for device k
$a_k(t)$	The number of packets arriving at device k from upper layer applications at time slot t
$d_k(t)$	Transmission selection metric at time slot t
λ_k	Data packet arrival rate for device k
L_k	Packet size of device k
$\mathbf{h}_k(t)$	The channel coefficient between device k and AP at time slot t
$\mathbf{w}(t)$	Energy beamforming vector at slot t
$\mathcal{H}_k(t)$	Energy harvested from AP by device k at time slot t
η	energy conversion efficiency
$n_k(t)$	Number of packets transmitted by device k at time slot t
$R_k(t)$	The link capacity between device k and the AP at time slot t
$E_k(t)$	Energy queue state of device k at time slot t
$Q_k(t)$	Data queue state of device k at time slot t
$\Psi(t)$	Virtual power queue state of the AP at time slot t
$A_k(t)$	AoI of device k at time slot t
$u_k(t)$	Timestamp of the latest packet of device k
\bar{P}_{AP}	Average transmit power of AP
P_{AP}^{max}	Peak transmit power of AP
P_k^{max}	Peak transmit power of device k
\hat{E}_k	Energy storage size of device k

where $P_k(t)$ and $x_k(t)$ are the transmit power and transmit signal, respectively. It is assumed that $\mathbb{E}[|x_k(t)|^2] = 1$. $\mathbf{z}_{AP,k}(t) \in \mathbb{C}^{N \times 1}$ denotes the additive white Gaussian noise at AP and $\mathbf{z}_{AP,k}(t) \sim \mathcal{CN}(0, \mathbf{I}_N \sigma^2)$, where \mathbf{I}_N is the identity matrix of $N \times N$. Let $n_k(t)$ represent the number of packets successfully transmitted from device k to AP, while the indicator function of $I_k(t) \in \{0, 1\}$ is used to indicate whether the AP can successfully receive $n_k(t)$ packets when device k is scheduled for transmissions, thus $I_k(t)$ can be given by

$$I_k(t) = \begin{cases} 1, & \text{if } d_k(t)R_k(t) \geq n_k(t)L_k, \\ 0, & \text{otherwise.} \end{cases} \quad (6)$$

Let $R_k(t)$ represent the link capacity (*bits/slot*) (the maximal amount of data (unit: bits) that can be reliably transmitted from device k to AP) at time slot t , and

$$R_k(t) = B \log_2 \left(1 + \frac{P_k(t)\|\mathbf{h}_k(t)\|^2}{\sigma^2} \right), \quad (7)$$

where B represents the channel bandwidth allocated to every device, we assume unity time slot duration. It should be stressed that, multi-packet transmission is considered in this paper, namely, the scheduled device can transmit as many packets to the AP as possible within the uplink capacity limit, namely, $n_k(t) = \lfloor R_k(t)/L_k \rfloor$, where $\lfloor \cdot \rfloor$ stands for the rounding down operation.

C. Energy Storage and Data Buffer Update

Each device can store the collected energy in its energy storage in the downlink RF energy transfer mode. When device

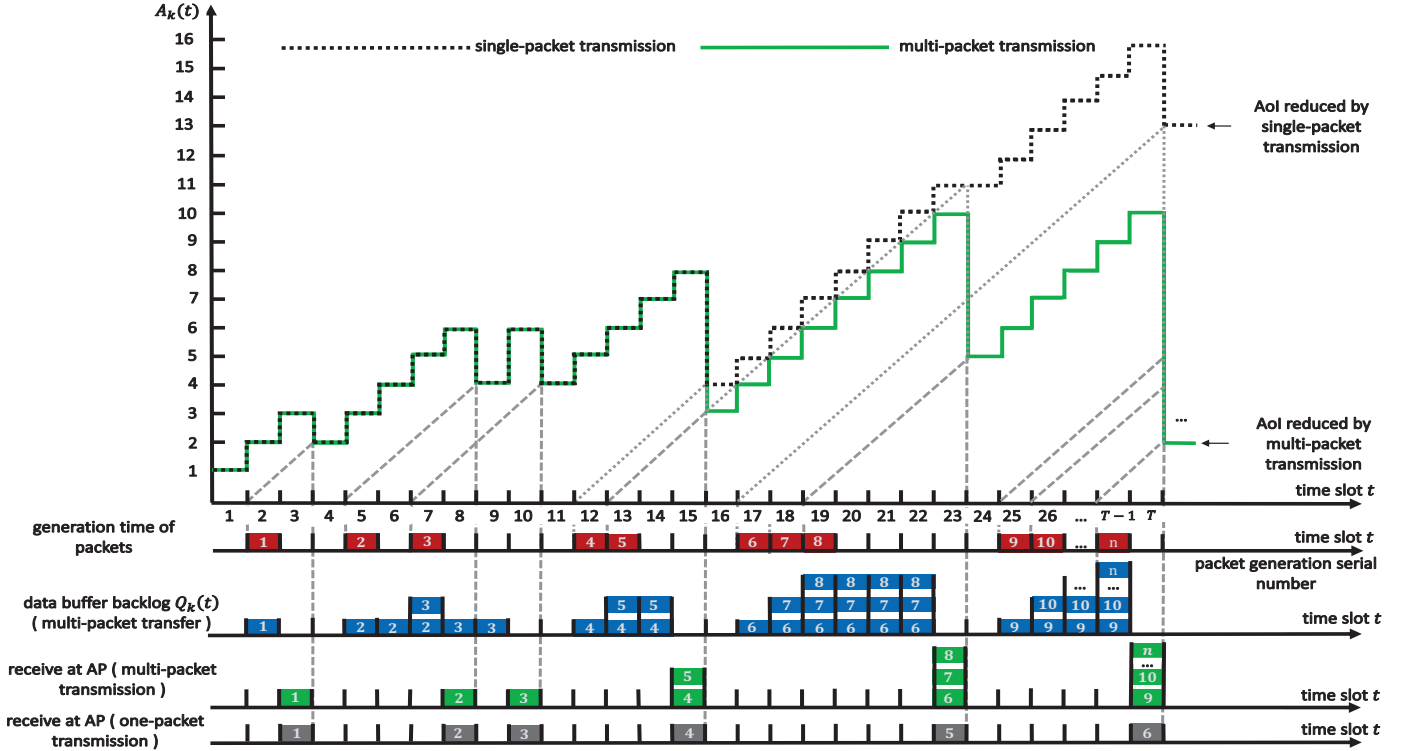


Fig. 2. AoI evolution example with fixed single packet transmission and adaptive multiple packet transmission in the buffer-aided wireless powered IoT network.

k is scheduled for the uplink transmission, it will first extract packets from its data buffer and then transmit the fresh packets to the AP by using the harvested energy. The energy storage and data buffer updates can be characterized as below

$$E_k(t+1) = \min \left[(E_k(t) + \mathcal{H}_k(t) - d_k(t)P_k(t))^+, \hat{E}_k \right], \quad (8)$$

$$Q_k(t+1) = (Q_k(t) + a_k(t)L_k(t) - d_k(t)I_k(t)R_k(t))^+, \quad (9)$$

where \hat{E}_k represents the maximal energy storage size of device k and $(\cdot)^+ = \max\{\cdot, 0\}$.

D. Age of Information

Age of Information (AoI) refers to the time elapsed since the most recent data message was received by the destination, which can be used to measure the freshness of information from the perspective of the receiver. When the *FCFS* queuing rule is applied, the AoI evolution example for the k -th device is depicted in Fig. 2, where the fixed single packet transmission and adaptive multi-packet transmission are included for illustration. The associated data buffer backlog of device k by the end of each time slot with adaptive multi-packet transmission are presented as well. One may readily observe from Fig. 2 that, data packets at device k are generated in the 1st, the 5-th and the 7-th time slots, which are delivered to the AP in the 4-th, the 9-th and the 11-th time slots, respectively. In addition, the difference in AoI performance between adaptive multi-packet transmission strategy and fixed single packet transmission strategy can be shown in time slots 16, 24, and T . Let $u_k(t)$ denote the generation time of the latest data packet received by AP from device k in time slot t , the AoI measure $A_k(t)$ of device k can thus be given by

$$A_k(t) = \begin{cases} t - u_k(t), & \text{if } d_k(t) = 1, I_k(t) = 1 \\ A_k(t-1) + 1, & \text{otherwise.} \end{cases} \quad (10)$$

Like [43] and [44], the average AoI metric is used in this paper to characterize the achievable AoI performance of a specific device k , which can be denote by:

$$\bar{A}_k = \lim_{T \rightarrow \infty} \frac{1}{T} \sum_{t=0}^{T-1} A_k(t). \quad (11)$$

Like [24], [45], and [46], we use the following average weighted AoI metric to evaluate the overall achievable AoI performance of the system:

$$\bar{A} = \lim_{T \rightarrow \infty} \frac{1}{TK} \sum_{t=0}^{T-1} \sum_{k=1}^K \theta_k A_k(t), \quad (12)$$

where θ_k stands for the AoI priority level of device k , $\theta_k \in [0, 1]$ and $\sum_{k=1}^K \theta_k = 1$.

E. Problem Formulation

In this paper, our objective is to minimize the average weighted AoI of wireless powered IoT network subject to data buffer and energy storage causal constraints, transmission mode selection constraint, peak and average transmit power

constraints of the AP, which can be summarized as follows:

$$\begin{aligned}
\mathbf{P1} : & \min_{\mathbf{w}(t), \mathbf{P}(t), \mathbf{n}(t), \mathbf{d}(t)} : \lim_{T \rightarrow \infty} \frac{1}{TK} \sum_{t=0}^{T-1} \sum_{k=1}^K \theta_k A_k(t) \\
\text{C1} : & E_k(t+1) = \min \left[(E_k(t) + \mathcal{H}_k(t) - d_k(t)P_k(t))^+, \hat{E}_k \right], \forall k, t, \\
\text{C2} : & d_k(t) \in \{0, 1\}, \forall k, t \\
\text{C3} : & \sum_{k=0}^K d_k(t) = 1, \forall t \\
\text{C4} : & I_k(t) = \begin{cases} 1, & \text{if } d_k(t)R_k(t) \geq n_k(t)L_k, \\ 0, & \text{otherwise,} \end{cases} \forall k, t, n_k(t) \in N^+, \\
\text{C5} : & A_k(t) = \begin{cases} t - u_k(t), & \text{if } d_k(t)=1, I_k(t)=1, \\ A_k(t-1) + 1, & \text{otherwise,} \end{cases} \forall k, t, \\
\text{C6} : & 0 \leq d_k(t)P_k(t) \leq \min[E_k(t), P_k^{\max}], \forall k, t, \\
\text{C7} : & Q_k(t+1) = (Q_k(t) + a_k(t)L_k(t) - d_k(t)I_k(t)R_k(t))^+, \forall k, t, \\
\text{C8} : & \lim_{T \rightarrow \infty} \frac{1}{T} \sum_{t=0}^{T-1} d_k(t)I_k(t)R_k(t) \geq \lambda_k L_k, \forall k, t, \\
\text{C9} : & \lim_{T \rightarrow \infty} \frac{1}{T} \sum_{t=0}^{T-1} d_0(t) \|\mathbf{w}(t)\|^2 \leq \bar{P}_{AP}, \forall t, \\
\text{C10} : & d_0(t) \|\mathbf{w}(t)\|^2 \leq P_{AP}^{\max}, \forall t,
\end{aligned}$$

where P_k^{\max} is the peak transmit power of device k , \bar{P}_{AP} and P_{AP}^{\max} are the maximal average transmit power and peak transmit power of the AP, respectively. C1 represents the energy queue causal constraint. C2 and C3 stand for the transmission mode selection constraints. C4 is the device transmission rate constraint. C5 is the AoI evolution constraint. C6 is the device peak transmit power constraint. C7 is the data queue evolution constraint. C8 specifies that the average departure rate of every device is no less than its generation rate to retain the stability of the data buffer. C9 and C10 are the average transmit power constraint and the peak transmit power constraints of the AP in the downlink RF energy transfer mode, respectively. In $\mathbf{P1}$, energy beams $\mathbf{w}(t)$, power allocation $\mathbf{P}(t) = (P_1(t), P_2(t), \dots, P_K(t))$ at all K devices, the number of transmitted status update packets $\mathbf{n}(t) = (n_1(t), n_2(t), \dots, n_K(t))$, and transmission mode selection $\mathbf{d}(t) = (d_0(t), d_1(t), \dots, d_K(t))$ are jointly optimized to minimize the long-term average weighted AoI.

III. ADAPTIVE AOI-AWARE TRANSMISSION DESIGN

Obviously, $\mathbf{P1}$ is a non-convex mixed-integer optimization problem, which is difficult to be solved directly. In this subsection, we will utilize the Lyapunov optimization framework to transform the time-averaging constraint into a queueing stability requirement. On this basis, we can derive the adaptive AoI-aware wireless transmission scheme. Let us define a virtual energy consumption queue $\Psi(t)$ of the AP in C9, and its status update can be given as follows

$$\Psi(t+1) = (\Psi(t) + d_0(t) \|\mathbf{w}(t)\|^2 - \bar{P}_{AP})^+, \forall t. \quad (13)$$

As for data queue $Q_k(t)$ and virtual energy consumption queue $\Psi(t)$, we have the following theorem.

Theorem 1: If data queue $Q_k(t)$ and virtual energy consumption queue $\Psi(t)$ are rate stable, i.e., $\lim_{T \rightarrow \infty} \frac{Q_k(T)}{T} = \lim_{T \rightarrow \infty} \frac{\Psi(T)}{T} = 0$, we have the following relationship:

$$\lim_{T \rightarrow \infty} \frac{1}{T} \sum_{t=0}^{T-1} d_k(t) I_k(t) R_k(t) \geq \lambda_k L_k \quad (14)$$

$$\lim_{T \rightarrow \infty} \frac{1}{T} \sum_{t=0}^{T-1} d_0(t) \|\mathbf{w}(t)\|^2 \leq \bar{P}_{AP} \quad (15)$$

Proof. Please see Appendix A. \square

According to *Theorem 1*, one can readily find out that, if the virtual energy consumption queue is rate stable, the time-averaged power consumption constraint of the AP can be satisfied. This implies that, the time-averaged power consumption constraint can be equivalently transformed to a stability problem of the virtual energy consumption queue. Hence, the original time-averaged optimization problem $\mathbf{P1}$ is equivalent to minimizing the average weighted AoI problem under the constraint of the virtual energy consumption queue stability, which can be solved by using the Lyapunov optimization framework.

Let $\Theta(t) = [Q_k(t), E_k(t), \Psi(t)]$ denote the state vector of all involved queues in time slot t . According to the status of data buffer, energy storage, and virtual energy consumption queue in time slot t , we can construct the following quadratic Lyapunov function:

$$\begin{aligned}
L(\Theta(t)) = & \frac{1}{2} \sum_{k=1}^K \left\{ \mu_{Q,k} Q_k^2(t) + \mu_{E,k} (\hat{E}_k - E_k(t))^2 \right\} \\
& + \frac{1}{2} \mu_0 \Psi^2(t)
\end{aligned} \quad (16)$$

where $\mu_{Q,k}, \mu_{E,k}, \mu_0$ are the weighting coefficients utilized to make the magnitudes of all queue states comparable. In order to guarantee the stability of all queues, we introduce the following Lyapunov shift to represent the variation of Lyapunov function between two consecutive time slots:

$$\Delta(\Theta(t)) = \mathbb{E}[L(\Theta(t+1)) - L(\Theta(t)) | \Theta(t)] \quad (17)$$

where $\mathbb{E}[\cdot]$ specifies the statistical expectation of the randomness of CSI and the dynamic choices of transmission modes given $\Theta(t)$. Since our goal is to minimize the average weighted AoI, we can construct the following Lyapunov drift-plus-penalty:

$$\Delta(\Theta(t)) + V \mathbb{E} \left[\sum_{k=1}^K \theta_k A_k(t+1) \mid \Theta(t) \right] \quad (18)$$

where V is a non-negative weighting coefficient that is employed to adjust the tradeoff between the average weighted AoI of the system and the queueing size, which we will refer it to as AoI weighting coefficient as well. By minimizing the above Lyapunov drift-plus-penalty function, the minimization of average weighted AoI and the stability of all queues can be achieved simultaneously.

Theorem 2: The upper bound of the Lyapunov drift-plus-penalty function is given by:

$$\begin{aligned} & \Delta(\Theta(t)) + V \mathbb{E} \left[\sum_{k=1}^K \theta_k A_k(t+1) \mid \Theta(t) \right] \\ & \leq C_0 + \sum_{k=1}^K \mathbb{E} \{ \mu_{Q,k} Q_k(t) (a_k(t) L_k - d_k(t) I_k(t) R_k(t)) \\ & \quad + \mu_{E,k} (\hat{E}_k - E_k(t)) (d_k(t) P_k(t) - \mathcal{H}_k(t)) \mid \Theta(t) \} \\ & \quad + \mu_0 \mathbb{E} [\Psi(t) (d_0(t) \|\mathbf{w}(t)\|^2 - \bar{P}_{AP}) \mid \Theta(t)] \\ & \quad + V \mathbb{E} \left[\sum_{k=1}^K \theta_k A_k(t+1) \mid \Theta(t) \right], \end{aligned} \quad (19)$$

where C_0 is a constant that is independent of all queues and V , and

$$\begin{aligned} C_0 = & \frac{1}{2} \sum_{k=1}^K \mu_{Q,k} (L_k^2 + \hat{R}_k^2) + \frac{1}{2} \sum_{k=1}^K \mu_{E,k} (\hat{\mathcal{H}}_k^2 + P_k^{\max 2}) \\ & + \frac{1}{2} \mu_0 (\bar{P}_{AP}^2 + P_{AP}^{\max 2}), \end{aligned} \quad (20)$$

where \hat{R}_k and $\hat{\mathcal{H}}_k$ denote the maximum transmission rate from device k to AP and the maximum energy harvested by device k in each time slot, respectively.

Proof. Please see Appendix B. \square

Adaptive AoI-aware transmission can be summarized in the following **Algorithm 1** table:

Based on *Theorem 2*, instead of minimizing the Lyapunov drift-plus-penalty function, we can minimize its upper bound. In each time slot t , according to current queue state $\Theta(t)$ and CSI, the upper bound can be minimized by optimizing energy beamforming vector $\mathbf{w}(t)$, data transmission power $P_k(t)$, transmitted packets number $n_k(t)$, and transmission modes $\mathbf{d}(t)$. Therefore, the optimization problem **P1** can be transformed into the following one:

$$\begin{aligned} \mathbf{P2} : & \min_{\mathbf{w}(t), \mathbf{P}(t), \mathbf{n}(t), \mathbf{d}(t)} : \sum_{k=1}^K \left\{ -\mu_{Q,k} Q_k(t) d_k(t) I_k(t) R_k(t) \right. \\ & \quad \left. + \mu_{E,k} (\hat{E}_k - E_k(t)) (d_k(t) P_k(t) - \mathcal{H}_k(t)) \right\} \\ & \quad + \mu_0 \Psi(t) d_0(t) \|\mathbf{w}(t)\|^2 + V \sum_{k=1}^K \theta_k A_k(t+1) \\ \text{s.t.} & \quad \text{C2, C3, C4, C6, and C10.} \end{aligned}$$

P2 is a mixed integer programming problem due to the transmission mode $d_k(t)$ ($k = 0, 1, 2, \dots, K$), which can be solved by enumerating $K+1$ cases. Specifically, we can derive the optimal energy beamforming vector by setting $d_0(t) = 1$. In the same way, we can obtain the optimal transmit power and the number of transmitted packets for device k by setting $d_k(t) = 1$ ($k \neq 0$). Namely, we can further decompose **P2** into $K+1$ different subproblems to separately derive the optimal energy beamforming, the optimal data transmission power allocation, the number of transmitted packets, as well as the optimal transmission mode selection.

Algorithm 1: Adaptive AoI-aware transmission

- 1: **Set** $\{t = 0 \mid t \in \{0, \dots, T-1\}\}$, **Input** $V, \bar{P}_{AP}, \{\lambda_k, \theta_k \mid k \in \{1, \dots, K\}\}$, and **Initialize** $\{Q_k(0) = 0, E_k(0) = 0, \Psi(0) = 0 \mid k \in \{1, \dots, K\}, t \in \{0, \dots, T-1\}\}$;
 - 2: **for** each time slot t , **Set** $\{d_k(t) = 0 \mid k \in \{0, \dots, K\}\}$ **do**
 - 3: solve the optimization problem

$$\begin{aligned} & \sum_{k=1}^K \{ \mu_{Q,k} Q_k(t) (a_k(t) L_k - d_k(t) I_k(t) R_k(t)) \\ & \quad + \mu_{E,k} (\hat{E}_k - E_k(t)) (d_k(t) P_k(t) - \mathcal{H}_k(t)) \} \\ & \quad + \mu_0 \Psi(t) (d_0(t) \|\mathbf{w}(t)\|^2 - \bar{P}_{AP}) + V \sum_{k=1}^K \theta_k A_k(t+1) \end{aligned}$$
 subject to C2, C3, C4, C6 and C10
 with variables $\mathbf{w}(t), \{P_k(t), n_k(t) \mid k \in \{1, \dots, K\}\}, \{d_k(t) \mid k \in \{0, \dots, K\}\}$
 - 4: **if** $\mathbf{w}(t) \mu_0 \Psi(t) \|\mathbf{w}(t)\|^2 - \sum_{k=1}^K \mu_{E,k} (\hat{E}_k - E_k(t)) \eta \mathcal{H}_k(t) + V \sum_{k=1}^K \theta_k (A_k(t) + 1) < \mu_{E,k} (\hat{E}_k - E_k(t)) P_k(t) - \mu_{Q,k} Q_k(t) I_k(t) R_k(t) + V \sum_{k=1}^K \theta_k A_k(t+1)$ **then**
 - 5: $d_0(t) = 1$, system work on **downlink RF energy transfer mode**;
 - 6: **else**
 - 7: $d_k(t) = 1, k \neq 0$, system work on **uplink data transmission mode**;
 - 8: **end if**
 - 9: **Update Queue Status** $\{Q_k(t+1), E_k(t+1), \Psi(t+1) \mid k \in \{1, \dots, K\}, t \in \{0, \dots, T-1\}\}$ and $\{\Psi(t+1) \mid t \in \{0, \dots, T-1\}\}$, set $t = t+1$ and return to step 2 until $t = T-1$
 - 10: **end for**
-

A. Optimal Energy Beamforming Design

When the system performs downlink energy harvesting, i.e., $d_0(t) = 1$, the optimization problem **P2** can be rewritten as:

$$\begin{aligned} \mathbf{P2.1} : & \min_{\mathbf{w}(t)} : \mu_0 \Psi(t) \|\mathbf{w}(t)\|^2 \\ & \quad - \sum_{k=1}^K \mu_{E,k} (\hat{E}_k - E_k(t)) \eta |\mathbf{h}_k^H(t) \mathbf{w}(t)|^2, \\ \text{s.t.} & \quad \|\mathbf{w}(t)\|^2 \leq P_{AP}^{\max}. \end{aligned}$$

P2.1 is a nonconvex problem, but we can solve it by converting it into a convex problem through the semi-positive definite relaxation (SDR) method. Let $\mathbf{S}(t) = \mathbf{w}(t) \mathbf{w}(t)^H$ and $\mathbf{B}(t) = \mathbf{h}_k(t) \mathbf{h}_k(t)^H$, we have $|\mathbf{h}_k^H(t) \mathbf{w}(t)|^2 = \text{tr}(\mathbf{B}(t) \mathbf{S}(t))$. Let $\mathbf{M}(t) = \mu_0 \Psi(t) \mathbf{I} - \sum_{k=1}^K \mu_{E,k} (\hat{E}_k - E_k(t)) \eta \mathbf{B}(t)$, where \mathbf{I} is the

identity matrix, **P2.1** can be equivalently transformed into:

$$\begin{aligned} \mathbf{P2.1.1} : \min_{\mathbf{S}(t)} &: \text{tr}(\mathbf{M}(t)\mathbf{S}(t)) \\ \text{s.t.} & 0 \leq \text{tr}(\mathbf{S}(t)) \leq P_{AP}^{\max}, \\ & \mathbf{S}(t) \succeq 0, \\ & \text{rank}(\mathbf{S}(t)) = 1. \end{aligned}$$

Since **P2.1.1** is convex, we can easily derive its optimal solution in *Theorem 3*.

Theorem 3: The optimal energy beamforming design is given by

$$\mathbf{w}^*(t) = \begin{cases} 0, & \text{if } \mathbf{M}(t) \succeq 0, \\ \sqrt{P_{AP}^{\max}} \mathbf{u}_1(t), & \text{otherwise,} \end{cases} \quad (21)$$

where $\mathbf{u}_1(t)$ is the eigenvector with respect to the smallest eigenvalue of $\mathbf{M}(t)$.

Proof. Please see Appendix C. \square

It should be noted that, the optimal energy beamforming design in (18) can guarantee $\Psi(t)$ satisfies *Theorem 1*, i.e., $\Psi(t)$ has the following upper bound:

$$\Psi(t) < \frac{\sum_{k=1}^K \mu_{E,k} (\hat{E}_k - E_k(t)) \eta \hat{h}_k^H}{\mu_0}. \quad (22)$$

Proof. Please see Appendix D. \square

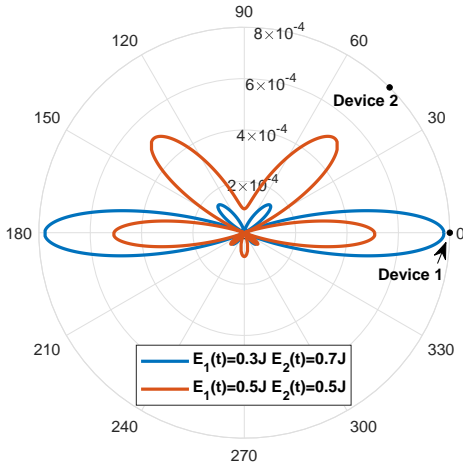


Fig. 3. Illustration of energy beamforming radiation with uniform array antenna, $N = 4$.

In Fig. 3, we present the radiation diagram of a uniform linear array antenna with $N = 4$ antenna to illustrate the relationship between the energy storage and the harvested energy. We take the energy beamforming design of two devices as an example, in which device 1 and device 2 are placed at 0° and 45° , respectively. As shown in Fig. 3, one can observe that: if $E_1(t) = E_2(t)$, both devices can receive almost the same energy beam; when $E_1 < E_2$, the main energy beam will be directed to device 1 such that it can harvest more energy.

B. Optimal Transmission Power and Rate Allocation

When the system selects the uplink data transmission mode, K devices will first extract fresh packets stored in their data buffer, and then send them to the AP in a TDMA manner. Without loss of generality, we assume that device k is scheduled in time slot t , i.e., $d_k(t) = 1$. In addition, in order to avoid wasting time resource, we expect that device k can successfully transmit $n_k(t)$ packets to the AP when it is scheduled, i.e., $I_k(t) = 1$. Therefore, by substituting them into **P2**, the optimization problem can be transformed as follows:

$$\begin{aligned} \mathbf{P2.2} : \min_{\mathbf{P}(t), \mathbf{n}(t)} &: \sum_{k=1}^K \left\{ -\mu_{Q,k} Q_k(t) n_k(t) L_k \right. \\ & \left. + \mu_{E,k} (\hat{E}_k - E_k(t)) P_k(t) \right\} + V \theta_k (t+1 - u_k(t)) \\ & + V \sum_{k' \neq k} \theta_{k'} (A_{k'}(t) + 1) \\ \text{s.t.} & B \log_2 \left(1 + \frac{P_k(t) \|\mathbf{h}_k^H(t)\|^2}{\sigma^2} \right) \geq n_k(t) L_k, \\ & 0 \leq P_k(t) \leq \min [E_k(t), P_k^{\max}]. \end{aligned}$$

Given the number of transmitted packets $n_k(t)$, the optimal transmit power is exactly equal to the power required to transmit $n_k(t)$ packets, which is given by

$$P_k^*(t) = \frac{\sigma^2 \left(2^{\frac{n_k(t) L_k}{B}} - 1 \right)}{\|\mathbf{h}_k^H(t)\|^2}. \quad (23)$$

Obviously, the maximum number of packets that can be sent to AP is dependent on the allowable peak transmit power, the energy storage state, and the data queue state. Therefore, the maximum possible transmitted packets by device k in time slot t is given by

$$\hat{n}_k(t) = \min \left\{ \frac{Q_k(t)}{L_k}, \left\lfloor \frac{B \log_2 \left(1 + \frac{\min [E_k(t), P_k^{\max}] \|\mathbf{h}_k^H(t)\|^2}{\sigma^2} \right)}{L_k} \right\rfloor \right\}, \quad (24)$$

where $\lfloor \cdot \rfloor$ is the rounding down operation. By substituting (23) and (24) into **P2.2**, we formulate the optimization problem as follows:

$$\begin{aligned} \mathbf{P2.2.1} : \min_{n_k(t)} &: \mu_{E,k} (\hat{E}_k - E_k(t)) \frac{\sigma^2 \left(2^{\frac{n_k(t) L_k}{B}} - 1 \right)}{\|\mathbf{h}_k^H(t)\|^2} \\ & - \mu_{Q,k} Q_k(t) n_k(t) L_k + V \theta_k (t+1 - u_k(t)) \\ & + V \sum_{k' \neq k} \theta_{k'} (A_{k'}(t) + 1) \\ \text{s.t.} & 0 \leq n_k(t) \leq \hat{n}_k(t). \end{aligned}$$

One can easily find out that, **P2.2.1** is a single-variable optimization problem of $n_k(t)$, which is an integer variable with upper bound $\hat{n}_k(t)$. In addition, it is worth noting that $u_k(t)$ is a function of $n_k(t)$, which is equal to the generation time of the latest packet among $n_k(t)$ packets. Therefore, we can obtain the optimal solution $n_k^*(t)$ to **P2.2.1** by exhaustively enumerating all possible numbers of packets sent by device k . Upon obtaining the optimal energy beamforming, the optimal transmit power, and the optimal number of transmitted packets, the optimal mode can be determined by substituting them into **P2**, i.e.,

$$d_k(t) = \begin{cases} 1, & \text{if } k = \arg \min_{k=0,1,2,\dots,K} \mathbb{I}_k(t), \\ 0, & \text{otherwise,} \end{cases} \quad (25)$$

where $\mathbb{L}_k(t)$ is the transmission mode selection metric given by

$$\begin{aligned} \mathbb{L}_0(t) &= V \sum_{k=1}^K \theta_k (A_k(t) + 1) + \mu_0 \Psi(t) \|\mathbf{w}^*(t)\|^2 \\ &\quad - \sum_{k=1}^K \mu_{E,k} \left(\hat{E}_k - E_k(t) \right) \eta \left| \mathbf{h}_k^H(t) \mathbf{w}^*(t) \right|^2, \quad (26) \\ \mathbb{L}_k(t) &= \mu_{E,k} \left(\hat{E}_k - E_k(t) \right) P_k^*(t) - \mu_{Q,k} Q_k(t) n_k^*(t) L_k \\ &\quad + V \theta_k (t+1 - u_k(t)) + V \sum_{k' \neq k} \theta_{k'} (A_{k'}(t) + 1), \quad k \neq 0. \quad (27) \end{aligned}$$

As we can see from mode selection metrics, when the system starts to operate, it first enters the downlink energy harvesting mode, where $E_k(t)$ gradually increases, so does $\mathbb{L}_0(t)$. On the other hand, the backlog $Q_k(t)$ gradually increases due to data arrival, thus reducing $\mathbb{L}_k(t)$. When the system enters the uplink data transmission mode, $Q_k(t)$ and $E_k(t)$ will decrease due to the energy consumption for data transmissions, so that $\mathbb{L}_0(t)$ decreases and $\mathbb{L}_k(t)$ increases. Therefore, as time goes by, the system will constantly switch between the downlink energy transmission mode and the uplink data transmission mode, making all queues enter stable states. In addition, we can note that, if a device has a larger backlog of the data queue and energy queue, which might lead to a smaller weighted sum AoI for the next slot when it is scheduled, the system tends to allocate transmission time slot to that device.

C. Queue Stability Analysis

In this section, we present an analysis of the stability of all queues. Since we consider the data generation mode with stochastic arrival and the *FCFS* queuing strategy without packet loss, the stability of the data queue $Q_k(t)$ can only be guaranteed for a specific range of status update rates λ_k . Therefore, it is necessary to ensure that the average output of $Q_k(t)$ are greater than the average input, i.e. Inequality (14) holds strictly.

Theorem 4: When (14) holds, there exists $\epsilon > 0$ such that $\lambda_k L_k + \epsilon \leq \mathbb{E}\{d_k(t)I_k(t)R_k(t) | \Theta(t)\}$ as well as $\mathbb{E}\{d_k(t)P_k(t) - \bar{H}_k(t) | \Theta(t)\} \leq -\epsilon$ strictly holds, then the data queue of the proposed adaptive AoI-aware transmission scheme is satisfied:

$$\begin{aligned} \lim_{T \rightarrow \infty} \frac{1}{T} \sum_{t=0}^{T-1} \sum_{k=1}^K \mathbb{E} \left\{ \mu_{Q,k} Q_k(t) + \mu_{E,k} \left(\hat{E}_k - E_k(t) \right) \right\} \\ \leq \frac{C_0 + V \sum_{k=1}^K \theta_k}{\epsilon} \quad (28) \end{aligned}$$

Proof. Please see Appendix E. \square

According to *Theorems 4* and (22), We can easily observe that the proposed AoI-aware transmission scheme is able to guarantee that all participating queues are strongly stable. This means that all data queues $Q_k(t)$ and energy queues $E_k(t)$ as well as virtual queue $\Psi(T)$ are rate stable [47]. Combined with *Theorem 1*, we know that as long as the status update rates λ_k of devices are controlled within the range where the data queue $Q_k(t)$ are stable, all packets arriving at $Q_k(t)$ can be successfully transmitted to AP.

IV. NUMERICAL RESULTS

In this section, we evaluate the performance of the proposed AoI-aware adaptive transmission scheduling scheme. The maximum energy storage size and the energy conversion efficiency are set to be $\hat{E}_k = 1$ J and $\eta = 0.25$, respectively. The transmission bandwidth allocated to each device and the noise variance at AP are assumed to be $B = 1000$ Hz and $\sigma^2 = -60$ dBm, respectively. Identical packet size of $L_k = 1500$ bits, $\forall k$ is assumed for all devices. In addition, the channel coefficient from device k to AP is modeled as $\mathbf{h}_k(t) = \sqrt{10^{-3} D_k^{-m}} \left[\alpha_{1,k}(t), \alpha_{2,k}(t) e^{jv_k}, \dots, \alpha_{N,k}(t) e^{j(N-1)v_k} \right]^T$, where D_k^m denotes the distance from device k to AP, m is the path loss factor, $\alpha_{i,k}(t)$ represents the short-term channel fading from device k to the i -th antenna of the AP, which is assumed to follow Rayleigh distribution with unit fading power gain. Unless otherwise stated, we assume $D_k = 5$ m and $m = 2$ in all numerical analysis. The phase difference between two successive antenna elements of device k is modeled as $v_k = -\frac{2\pi d_{is} \sin(\varphi_k)}{\xi}$, where ξ is the signal wavelength, d_{is} is the distance between two successive antenna elements, and φ_k is the direction from device k to AP. We assume that AP is equipped with four antennas (i.e., $N = 4$), and set $d_{is} = \xi/2$. The relationship between the average transmit power and the peak transmit power of the AP is set to be $P_{AP}^{max} = 5\bar{P}_{AP}$. Unless otherwise stated, we assume $\bar{P}_{AP} = 30$ dBm. The weighting coefficients of energy queue, data queue and virtual power consumption queue are set to be $\mu_{E,k} = 10^5$, $\mu_{Q,k} = 1$, and $\mu_0 = 10$, respectively. Unless otherwise stated, we assume the AoI weighting coefficient $V = 10$. All simulation results are obtained for 10^6 time slots.

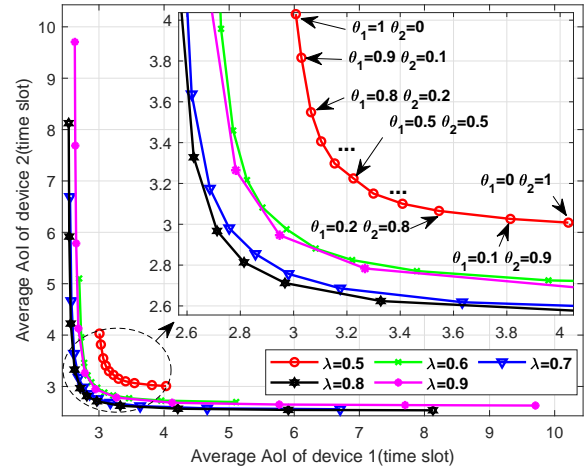


Fig. 4. Average achievable AoI regions for different status update rates, $K = 2$.

In Fig. 4, we illustrate the achievable average AoI region of two devices with different arrival rates. One can readily observe that, the AoI priority level θ_k has a significant impact on the realized average AoI performance. As expected, the device with a larger AoI priority level can realize a smaller AoI. This verifies the effectiveness of the AoI-aware design,

which enables the system to flexibly meet the AoI requirements of different devices by adjusting θ_k . In addition, one may also notice the impact of the status update rate on the achievable AoI region. It is shown that, when status update rate λ increases from 0.5 to 0.8, the achievable AoI region can be improved accordingly. With the further increase from 0.8 to 0.9, the achievable AoI region tends to degrade.

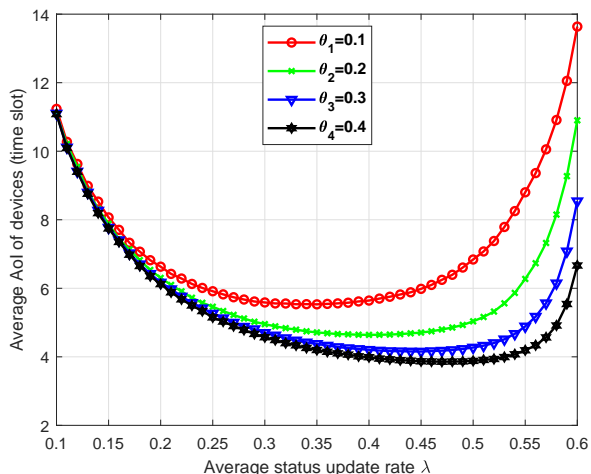


Fig. 5. The relationship between the average AoI and status update rate for devices with different AoI priority levels, $K = 4$.

In order to further show the status update rate and its influence on the realized average AoI performance, the average AoI performance of four devices is illustrated in Fig. 5. One can observe the influence of both status update rate and the AoI priority levels on the realized average AoI performance. Given $\lambda \in [0.1, 0.6]$, with the increase of status update rate, average AoI will first decrease until reaching its minimum value, and then gradually increases. Basically, there are three factors that affect the average AoI performance, namely, status update interval, queuing delay, and transmission latency. Because time division multiple access (TDMA) scheme is assumed, transmission delay will be one time slot for every device when scheduled for transmissions. Hence, status update interval and queuing delay will be two primary factors that affect the realized average AoI performance. This explicates the reason why the average AoI performance varies with the change in status update rate. As illustrated in Fig. 6, when status update rates of all devices are low (for instance, $\lambda = 0.1$), status update interval becomes the dominant factor, while queuing delays of all devices are small. As a result, all devices can achieve almost the same average AoI, even their AoI priority levels are different. As status update rate increases (for instance, $\lambda = 0.25$), status update interval decreases sharply, while queuing delay increases gradually, which explicates the improved average AoI performance by all devices. The minimal average AoI can be obtained at the crossing point when status update interval equals to queuing delay, as shown in Fig. 6. In fact, one may notice that, when status update rate is larger than the optimal status update rate point, queuing delay dominates the achieved average AoI performance. With the further increase in status update rate,

high status update rate incurs significant increase in queuing delay (for instance, $\lambda = 0.6$), which deteriorates the realized average AoI performance, as illustrated in Fig. 6. The above analysis shows us that, the task-related status update rate plays an important role in average AoI performance. There exists an optimal status update rate in terms of the realized minimum average AoI performance. The devices with a higher AoI priority level will have a larger optimal status update rate, this is because AoI-aware design tends to allocate more transmission opportunities to them such that their queuing delays increase more slowly.

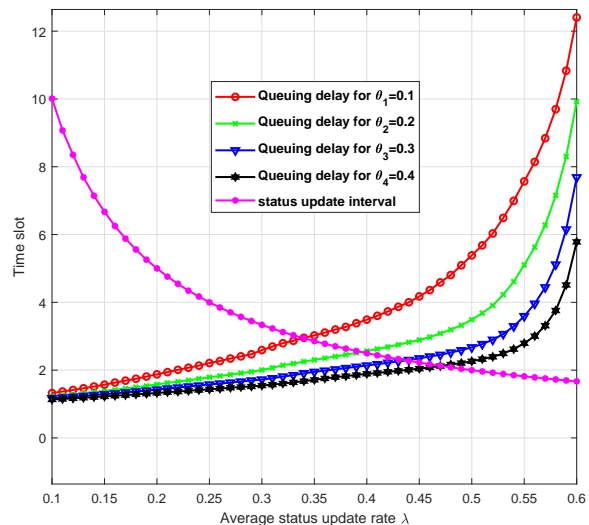


Fig. 6. Average packet queuing delay for devices with different AoI priority level θ_k and average status update rates, $K = 4$.

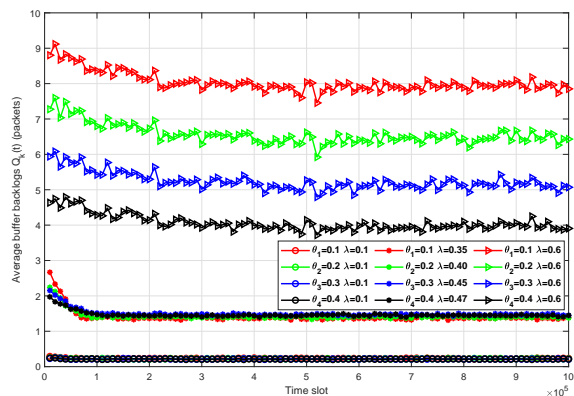


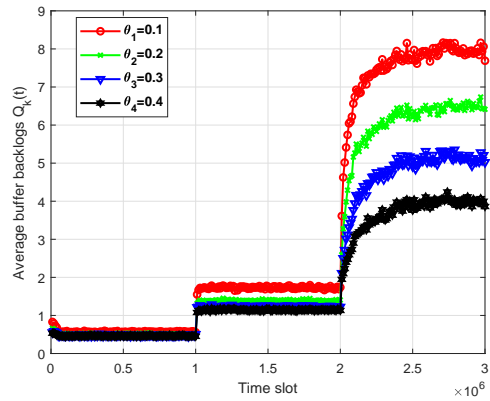
Fig. 7. Evolution of data buffer backlogs with different status update rates, $K = 4$.

In order to better illustrate the variation of queuing delay at devices, the data buffer backlog evolutions are illustrated in Fig. 7. One can readily find out that, within low status update rate region of $\lambda = 0.1$, the average backlogs of all devices are almost the same, which are less than one packet per time slot. In this case, status update interval dominates the average AoI performance, which concurs with our analysis

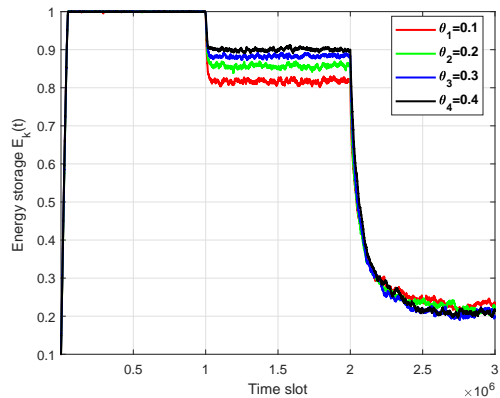
in Fig. 6. While within high status update rate region of $\lambda = 0.6$, one may notice obvious queue backlog at all devices. In fact, with the increase of status update rates, even the AoI-aware scheme manages to coordinate the transmission, the average data buffer backlog gradually tends to increase as well. Meanwhile, the devices with higher AoI priority levels will have smaller average buffer backlog, which indicates that the AoI-aware design is able to better meet the average AoI requirements. In this region, the queuing delay dominates the average AoI performance, therefore the devices with higher AoI priority level will have better average AoI performance, just as evidenced in Fig. 6. Interestingly, we can notice that the average buffer backlogs of four devices at their optimal status update rates (namely, $\lambda_1 = 0.34, \lambda_2 = 0.40, \lambda_3 = 0.45, \lambda_4 = 0.47$) are very close to each other, namely about 1.3 packet per time slot.

In order to further show the dynamic evolution characteristics of data buffer backlog $Q_k(t)$, the related energy storage $E_k(t)$, and energy consumption queue $\Psi_k(t)$, we demonstrate their dynamic evolutions in Fig. 8 for three status update rates of $\lambda = 0.2$ (the first one million time slots), $\lambda = 0.4$ (the second one million time slots), and $\lambda = 0.6$ (the last one million time slots), respectively. One can readily observe that, given the status update rate, the AoI-aware system can always reach some dynamic stability status in terms of data buffer backlog $Q_k(t)$, energy storage $E_k(t)$ and energy consumption queue $\Psi_k(t)$. On the one hand, when status update rate is low ($\lambda = 0.2$), there will be small backlog size and small energy consumption, since there is few status data generated and less energy is needed for transmission, which leads to a high energy storage level. On the other hand, when status update rate is high ($\lambda = 0.6$), there will be large data backlog size and high energy consumption for more status update transmission to AP, which gives rise to a low energy storage level. For moderate status update rate ($\lambda = 0.4$), most time slots will be allocated for data transmissions (as will be illustrated in Fig. 9), since the increase of status update rate will lead to some increase in buffer backlog. However, the virtual energy consumption queue $\Psi(t)$ is lower than that with low status update rate of $\lambda = 0.2$. This can be explained by the fact that data buffer has considerable backlog and devices have enough energy in their energy storages (i.e., $-\mu_{Q,k}Q_k(t)n_k^*(t)L_k$ has more weight than $\mu_{E,k}(\hat{E}_k - E_k(t))P_k^*(t)$ in Equ.(27)) when $\lambda = 0.4$. Systems tend to spend more time slots to transmit data to AP. In all cases, we notice the virtual energy consumption queue $\Psi(t)$ will reach a dynamic stability status, which verifies *Theorem 1*. Moreover, we can clearly notice the influence of AoI-aware design. The devices with a higher AoI priority level will have priority in data transmissions for the sake of minimizing the average AoI performance.

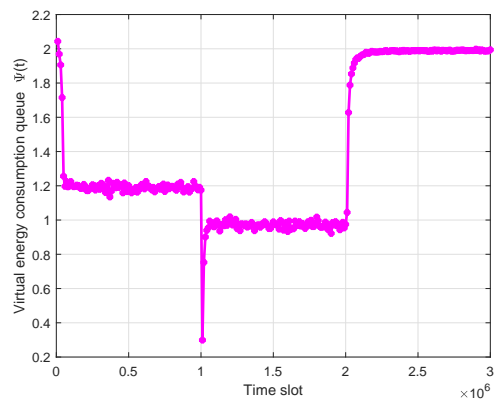
In order to clearly explicate the influence of AoI-aware design, we illustrate the percentages of energy harvesting and data transmissions for devices with a different AoI priority level θ_k in Fig. 9 for three status update rates of $\lambda = 0.2$, $\lambda = 0.4$ and $\lambda = 0.6$. One may note that, in all cases, the devices with higher AoI priority levels will always be allocated with more time slots in data transmissions. One



(a) Dynamic data buffer backlog evolution



(b) Dynamic energy storage evolution



(c) Dynamic energy consumption evolution

Fig. 8. The dynamic evolution of data buffer backlog, energy storage and virtual energy consumption queue, $K = 4$.

may observe that, for small status update rate of $\lambda = 0.2$, about 72% percentages of time slots will be allocated for data transmissions. Since the transmission load is low, there are enough time slots for both energy harvesting and data transmissions. In this case, 12% percentages of time slots are enough for energy harvesting. The rest 16% percentages of time slots will be wasted (neither for energy harvesting nor for data transmissions). For high status update rate of $\lambda = 0.6$, about 80% percentages of time slots are allocated for data transmissions, and the rest 20% percentages of time slots are

for energy harvesting. At this time, in order to alleviate the data buffer backlog, all devices will try to seize the communication opportunities to realize almost the same percentages of data transmissions for devices with a different AoI priority level θ_k . One can notice that, when status update rate (load) of the system is high, in addition to the time slots for energy harvesting, almost all the rest time slots will be used for data transmissions in order to reduce the average AoI, therefore, the energy storage is low, while both the buffer backlog size and the energy consumption are high, as illustrated in 8. Among three status update rates, the highest 89% percentage of time slots are allocated for data transmissions when $\lambda = 0.4$, while about 10.5% percentage of time slots are allocated for energy harvesting, the rest 0.5% percentages of time slots are wasted. Because now the load is larger than that with low load of $\lambda = 0.2$, there is small but noticeable buffer backlog size $Q_k(t)$ and smaller energy storage $E_k(t)$. However, since most time slots are allocated for data transmissions, the collected energy is still sufficient to support devices to transmit data with less energy consumption, as illustrated in 8. In addition, since the volume of data transmissions is larger at $\lambda = 0.6$ than at $\lambda = 0.2$ and $\lambda = 0.4$, its percentages of energy harvesting is also larger than at $\lambda = 0.2$ and $\lambda = 0.4$, as illustrated in Fig. 9.

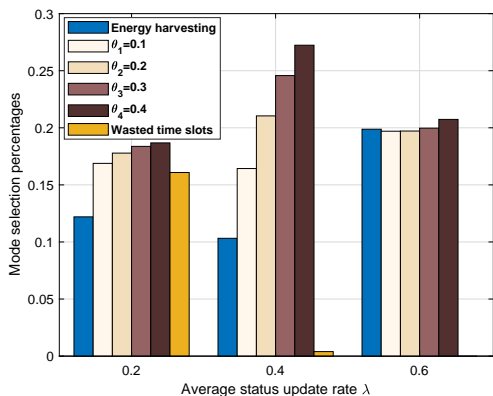


Fig. 9. The average mode selection percentages of energy harvesting and data transmission for devices with different AoI priority level θ_k , $K = 4$.

Because we consider the transmission subject to the channel capacity constraint C4 in optimization problem P1, multiple-packet transmission is allowed. The data transmission statistics of different devices are depicted in Fig. 10. One can readily observe that, the single packet transmission accounts for the majority in the low status update rate (light system load) region of $\lambda = 0.2$, while the multiple packet transmission will be the majority in the high status update rate (heavy system load) region of $\lambda = 0.6$. For the moderate status update rate of $\lambda = 0.4$, the single packet transmission will be the majority only for devices with a higher AoI priority level, while the multiple packet transmission becomes the majority for devices with a lower AoI preference. In fact, for those devices with a higher AoI preference, the AoI-aware system tries to schedule them to upload their data to the AP with priority. When the system load is low, the

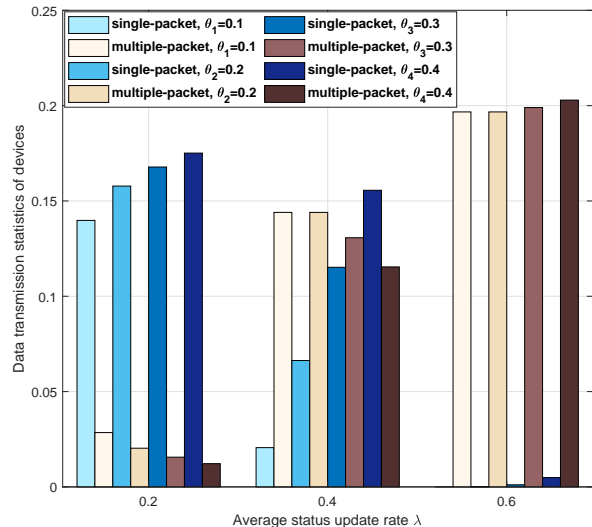


Fig. 10. The data transmission statistics of all devices with different AoI priority level θ_k , $K = 4$.

single packet transmission would suffice, which explicates the majority of the single packet transmission in the low status update rate region. On the other hand, when the system load becomes heavy, the multiple packet transmission will be more suitable, which explicates the majority within the high status update rate region. When the system load is neither small nor large, the devices with higher AoI preferences will have priority to upload their data to AP, resulting in more single packet transmissions. Of course, if all devices have AoI delivery requirements, the multiple packet transmissions are always needed, especially for those devices with lower AoI preferences. Those devices with a lower AoI priority will be scheduled in transmission with less priority, resulting in some increase of buffer backlog. Obviously, the multiple packet transmission is more effective in terms of quickly eliminating buffer backlog when the underlying channel quality allows.

All the above analysis results indicate that, the AoI-aware system can serve devices with different average AoI requirements by setting an appropriate AoI priority level θ_k , $k \in [1, K]$. In addition to the AoI priority level, weighting coefficient V is employed in (18) to adjust the tradeoff between the average weighted AoI and the incurred queueing size. In order to highlight the influence of V on the realized average weighted AoI performance, let us focus on the realized average weighted AoI performance with homogeneous AoI requirements (*i.e.*, $\theta_k = \frac{1}{K}$). In Fig. 11 we illustrate the realized average weighted AoI performance with different V for a high status update rate region of $\lambda = 0.6$. One may readily observe from Fig. 11 that, there exists a reasonable choice of V in terms of the achievable average weighted AoI performance. In fact, when V is very small (for instance, $V = 0$), the AoI-aware system will not put emphasis on average weighted AoI, instead, the average data buffer, energy storage, and virtual energy consumption will be addressed, which makes the system activate the downlink RF energy transfer mode

instead of the uplink data transmission mode. As illustrated in Fig. 12 and Fig. 13, a small V will lead to large energy storage E_k and large data buffer backlog size. Consequently, the resultant average weighted AoI performance is not ideal. On the other hand, when V is large (for instance, $V = 16$), the AoI-aware system will put more emphasis on the average weighted AoI performance, which makes the system select the uplink data transmission mode instead of the downlink RF energy transfer mode. Consequently, the resultant harvested energy is low, which will affect the uplink data transmission. As illustrated in Fig. 13, if $V > 16$, the realized average weighted AoI performance will degrade sharply. We may conclude from Fig. 11- Fig. 13 that, the AoI-aware design should consider an appropriate setting of V .

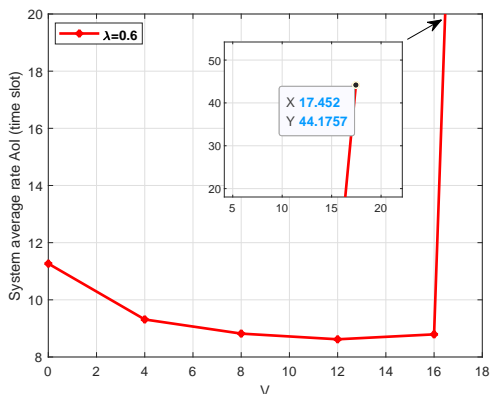


Fig. 11. The influence of weighting coefficient V on the realized average weighted AoI performance, $K = 4$.

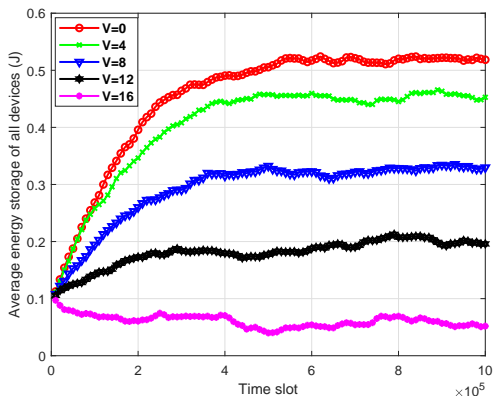


Fig. 12. Average energy storage evolution with different weighting coefficient V , $\lambda = 0.6$.

Finally, in order to demonstrate the performance gain achieved by the proposed AoI-aware design, we show the realized average weighted AoI performance in Fig. 14, in which several benchmark schemes are included for comparisons. More specifically, the following schemes are utilized as the benchmarks: the first one is the adaptive scheme with a fixed number of transmission packet, which can be derived by solving problem **P2** with a fixed number of transmitted packets $n_k(t)$, (we consider three cases of $n_k(t) = 1$,

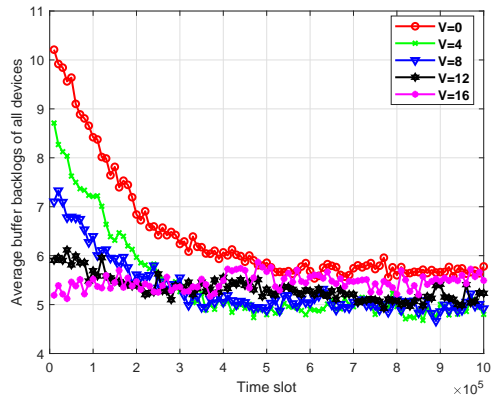


Fig. 13. Data buffer backlog evolution with different weighting coefficient V , $\lambda = 0.6$.

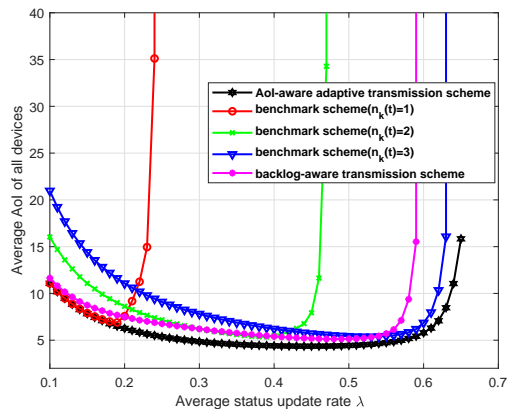


Fig. 14. The realized average weighted AoI performance with different status update rates.

$n_k(t) = 2$, and $n_k(t) = 3$); the second one is the backlog-aware transmission scheme, which can be derived by solving problem **P2** but considering only data buffer backlog (i.e., $-\mu_{Q,k}Q_k(t)n_k^*(t)L_k$ in (27)). One can see that the proposed AoI-aware adaptive transmission scheme outperforms two benchmark schemes in terms of the realized average weighted AoI performance. In fact, with the increase in status update rate λ , the proposed AoI-aware transmission scheme can support higher status update rates with a reasonable average weighted AoI performance. As illustrated in Fig. 10, the proposed AoI-aware transmission scheme can adaptively adjust the number of packets transmitted in each time slot according to current BSI, ESI, CSI and ASI, which enables it to fully utilize the underlying communication resources to achieve the best average weighted AoI for the given status update rates. In addition, backlog-aware transmission scheme only considers the BSI, so as to ensure the fairness among different devices, but it neglects the potential average weighted AoI performance gains owing to the rational scheduling on the basis of the underlying CSI, ESI and ASI.

V. CONCLUSION REMARKS

In this paper, we considered an AoI-aware status update in a buffer-aided wireless powered IoT network, where an AP provides energy to all IoT devices through downlink energy transfer, and all devices transmit their traffic-related status update data to the AP in a TDMA manner by utilizing the harvested energy. Firstly, the energy beamforming vectors, the power allocation, the number of transmitted packets, and the device scheduling scheme were jointly considered in the proposed adaptive AoI-aware transmission scheme to minimize the average weighted AoI. Secondly, in order to handle the proposed time-averaged optimization problem, we transformed the time-averaged optimization problem into a real-time one under the Lyapunov optimization framework, which can be further decomposed into several subproblems to derive the adaptive AoI-aware transmission scheme. Numerical results have been presented to unveil that status update rates of devices can directly affect the realized average AoI performance. In addition, our analysis disclosed that the priority level and AoI metric related weighting coefficient should be carefully selected to better meet the AoI requirements. Finally, how to fulfill the timely status update requirements in heterogenous channel conditions, how to serve heterogenous traffic requirements (guaranteeing the timely status update traffic while accommodating those latency insensitive traffic), how to further improve the AoI performance by considering NOMA techniques, will be left for our future work.

APPENDIX A

Based on (9) and (13), we have

$$Q_k(t+1) \geq Q_k(t) + a_k(t)L_k(t) - d_k(t)I_k(t)R_k(t), \quad (29)$$

$$\Psi(t+1) \geq \Psi(t) + d_0(t)\|\mathbf{w}(t)\|^2 - \bar{P}_{AP}, \quad (30)$$

By summing (29) and (30) from $t = 0$ to $t = T - 1$ and dividing by T , and taking the limit on both side, we have

$$\lim_{T \rightarrow \infty} \frac{Q_k(T) - Q_k(0)}{T} \geq \lambda_k L_k - \lim_{T \rightarrow \infty} \frac{1}{T} \sum_{t=0}^{T-1} d_0(t)I_k(t)R_k(t), \quad (31)$$

$$\lim_{T \rightarrow \infty} \frac{\Psi(T) - \Psi(0)}{T} \geq \lim_{T \rightarrow \infty} \frac{1}{T} \sum_{t=0}^{T-1} (d_0(t)\|\mathbf{w}(t)\|^2 - \bar{P}_{AP}), \quad (32)$$

Without loss of generality, we assume that data queues and the virtual power consumption queue initial state are set to be zero. Thus, if data queues and the virtual power consumption queue are rate stable, i.e., $\lim_{T \rightarrow \infty} \frac{Q_k(T)}{T} = \lim_{T \rightarrow \infty} \frac{\Psi(T)}{T} = 0$, by substituting it into (31) and (32), we obtain Theorem 1.

APPENDIX B

Based on (8), (9), and (13), we have

$$\begin{aligned} & (\hat{E}_k - E_k(t+1))^2 - (\hat{E}_k - E_k(t))^2 \\ & \leq 2(\hat{E}_k - E_k(t))(d_k(t)P_k(t) - \mathcal{H}_k(t)) + \hat{\mathcal{H}}_k^2 + P_k^{\max 2}, \end{aligned} \quad (33)$$

$$\begin{aligned} & Q_k(t+1)^2 - Q_k(t)^2 \\ & \leq 2Q_k(t)(a_k(t)L_k - d_k(t)I_k(t)R_k(t)) + L_k^2 + \hat{R}_k^2, \end{aligned} \quad (34)$$

$$\begin{aligned} & \Psi(t+1)^2 - \Psi(t)^2 \\ & \leq 2\Psi(t)(d_0(t)\|\mathbf{w}(t)\|^2 - \bar{P}_{AP}) + \bar{P}_{AP}^2 + P_{AP}^{\max 2}. \end{aligned} \quad (35)$$

Since the arrival process of each packet is assumed to follow the Bernoulli process, at most one packet arrives per slot. Thus, we have $(a_k(t)L_k)^2 \leq L_k^2$. By substituting above inequalities into (18), we obtain Theorem 2.

APPENDIX C

Since matrix $\mathbf{S}(t)$ is semi-positive definite and $\text{rank}(\mathbf{S}(t)) = 1$. Therefore, the eigenvalue decomposition of matrices $\mathbf{S}(t)$ and $\mathbf{M}(t)$ yields

$$\mathbf{S}(t) = \mathbf{V}(t)\boldsymbol{\Sigma}_S(t)\mathbf{V}(t)^H, \quad (36)$$

$$\mathbf{M}(t) = \mathbf{U}(t)\boldsymbol{\Sigma}_M(t)\mathbf{U}(t)^H, \quad (37)$$

where $\boldsymbol{\Sigma}_S(t) = \text{diag}(s_1(t), 0, \dots, 0)$ and $s_1(t) \geq 0$, $\boldsymbol{\Sigma}_M(t) = \text{diag}(m_1(t), m_2(t), \dots, m_N(t))$ are diagonal matrices, and $\mathbf{V}(t)$ and $\mathbf{U}(t)$ are unitary matrices. Therefore, we have

$$\begin{aligned} \text{tr}(\mathbf{M}(t)\mathbf{S}(t)) &= \text{tr}(\mathbf{U}(t)\boldsymbol{\Sigma}_M(t)\mathbf{U}(t)^H\mathbf{V}(t)\boldsymbol{\Sigma}_S(t)\mathbf{V}(t)^H) \\ &= \text{tr}(\mathbf{V}(t)^H\mathbf{U}(t)\boldsymbol{\Sigma}_M(t)\mathbf{U}(t)^H\mathbf{V}(t)\boldsymbol{\Sigma}_S(t)). \end{aligned} \quad (38)$$

Let matrix $\mathbf{T}(t) = \mathbf{U}(t)^H\mathbf{V}(t)$, then $\text{tr}(\mathbf{M}(t)\mathbf{S}(t)) = \text{tr}(\mathbf{T}(t)^H\boldsymbol{\Sigma}_M(t)\mathbf{T}(t)\boldsymbol{\Sigma}_S(t)) = s_1(t)\sum_{i=1}^N m_i(t)|t_{i1}|^2$, where $(t_{11}(t), t_{21}(t), \dots, t_{N1}(t))^T$ is the column vector of the first column of matrix $\mathbf{T}(t)$. Since $\mathbf{T}(t)$ is a unitary matrix, we have $\sum_{i=1}^N |t_{i1}|^2 = 1$. The following can be sub-divided into two cases:

If $0 \leq m_1(t) \leq m_2(t) \leq \dots \leq m_N(t)$, we have $\text{tr}(\mathbf{M}(t)\mathbf{S}(t)) \geq 0$, the objective function $\text{tr}(\mathbf{M}(t)\mathbf{S}(t))$ has a minimum value of 0, when $\mathbf{w}(t) = 0$.

If $m_1(t) \leq m_2(t) \leq \dots \leq m_N(t) \leq 0$, we have, $\text{tr}(\mathbf{M}(t)\mathbf{S}(t)) = s_1(t)\sum_{i=1}^N m_i(t)|t_{i1}|^2 \geq m_1(t)s_1(t) \geq m_1(t)P_{AP}^{\max}$, when $\mathbf{U}(t) = \mathbf{V}(t)$ and $s_1(t) = P_{AP}^{\max}$, the equality holds, then $\mathbf{S}(t) = \mathbf{U}(t)\boldsymbol{\Sigma}_S(t)\mathbf{U}(t)^H = P_{AP}^{\max}\mathbf{u}_1(t)\mathbf{u}_1^H(t)$, where $\mathbf{u}_1(t)$ is the eigenvector corresponding to the smallest eigenvalue in the matrix $\mathbf{M}(t)$, then $\mathbf{w}(t) = \sqrt{P_{AP}^{\max}}\mathbf{u}_1(t)$. Proof of Theorem 3 is completed.

APPENDIX D

Let

$$\mathcal{L} = \mu_0\Psi(t)\|\mathbf{w}(t)\|^2 - \sum_{k=1}^K \mu_{E,k}(\hat{E}_k - E_k(t))\eta\|\mathbf{h}_k^H(t)\mathbf{w}(t)\|^2.$$

When $\|\mathbf{w}(t)\|^2 = 0$, then $\mathcal{L} = 0$. We have $\mathcal{L}_{\min} \leq \mathcal{L} = 0$. Based on the Cauchy-Schwarz inequality, we have:

$$\begin{aligned} \mathcal{L}_{\min} &\geq \\ &\left[\mu_0\Psi(t) - \sum_{k=1}^K \mu_{E,k}(\hat{E}_k - E_k(t))\eta\|\mathbf{h}_k^H(t)\|^2 \right] \|\mathbf{w}(t)\|^2 \geq \\ &\left[\mu_0\Psi(t) - \sum_{k=1}^K \mu_{E,k}(\hat{E}_k - E_k(t))\eta\hat{h}_k^H \right] \|\mathbf{w}(t)\|^2 \end{aligned} \quad (39)$$

If $\mu_0\Psi(t) \geq \sum_{k=1}^K \mu_{E,k}(\hat{E}_k - E_k(t))\eta\hat{h}_k^H$, we have $\mathbf{w}(t) = 0$ and $\mathcal{L}_{\min} = 0$.

If $\mu_0\Psi(t) < \sum_{k=1}^K \mu_{E,k}(\hat{E}_k - E_k(t))\eta\hat{h}_k^H$, we have $\mathbf{w}(t) = \frac{\sqrt{P_{AP}^{\max}}\mathbf{u}_1(t)}{\sum_{k=1}^K \mu_{E,k}(\hat{E}_k - E_k(t))\eta\hat{h}_k^H}$ and $\mathcal{L}_{\min} < 0$ and $\Psi(t) < \frac{\sum_{k=1}^K \mu_{E,k}(\hat{E}_k - E_k(t))\eta\hat{h}_k^H}{\mu_0}$. Thus $\Psi(t)$ has an upper bound.

APPENDIX E

For the optimization problem **P1**, if (14), $\mathbb{E}\{d_k(t)P_k(t)\} \leq \mathbb{E}\{\mathcal{H}_k(t)\}$ and (15) are constant hold, then there exists a random stochastic strategy such that the following inequality holds:

$$\mathbb{E}\{a_k(t)L_k - d_k(t)I_k(t)R_k(t) \mid \Theta(t)\} \leq -\epsilon \quad (40)$$

$$\mathbb{E}\{d_k(t)P_k(t) - \mathcal{H}_k(t) \mid \Theta(t)\} \leq -\epsilon \quad (41)$$

$$\mathbb{E}\{d_0(t)\|\mathbf{w}(t)\|^2 - \bar{P}_{AP} \mid \Theta(t)\} \leq -0 \quad (42)$$

Turn (10) into the following expression:

$$A_k(t+1) = \left(1 - d_k(t)I_k(t)\right) (A_k(t) + 1) + d_k(t)I_k(t) \left(t + 1 - u_k(t)\right) \quad (43)$$

Take (40), (41), (42) and (43) into (18), we can get:

$$\begin{aligned} \Delta(\Theta(t)) + V\mathbb{E}\left[\sum_{k=1}^K \theta_k A_k(t+1) \mid \Theta(t)\right] \\ \leq C_0 - \epsilon \sum_{k=1}^K \left[\mu_{Q,k}Q_k(t) + \mu_{E,k}(\hat{E}_k - E_k(t))\right] \\ + V \sum_{k=1}^K \theta_k \left\{ \underbrace{\left(t - u_k(t) - A_k(t)\right)}_{\leq 0} \mathbb{E}[d_k(t)I_k(t) \mid \Theta(t)] + A_k(t) + 1 \right\} \end{aligned} \quad (44)$$

By taking the expectation of (44) and summing from $t = 0$ to $t = T - 1$ and dividing by T , we have

$$\begin{aligned} \frac{L(\Theta(T)) - L(\Theta(0))}{T} + V \sum_{k=1}^K \theta_k \frac{A_k(T) - A_k(0)}{T} \\ \leq C_0 + V \sum_{k=1}^K \theta_k - \frac{\epsilon}{T} \sum_{t=0}^{T-1} \sum_{k=1}^K \left[\mu_{Q,k}Q_k(t) + \mu_{E,k}(\hat{E}_k - E_k(t))\right] \end{aligned} \quad (45)$$

Without loss of generality, we assume that the initial state of all queues is 0, i.e. $L(\Theta(0)) = 0$, and the AoI of the initial time slot of all devices is 1, that is, $A_k(0) = 1$. At the same time, since $L(\Theta(T)) \geq 0$ and $A_k(T+1) \geq 0$, (28) can be obtained for $T \rightarrow \infty$ in (45). Thus the joint queue state is stable within the allowable range of λ_k .

REFERENCES

- [1] A. Gohar and G. Nencioni, "The Role of 5G Technologies in a Smart City: The Case for Intelligent Transportation System," *Sustainability*, 13 (2021): 5188.
- [2] M. Q. Aldossari and A. Sidorova, "Consumer Acceptance of Internet of Things (IoT): Smart Home Context," *Journal of Computer Information Systems*, 60 (2020): 507 - 517.
- [3] Y. Cheng, et al, "Research on the Smart Medical System Based on NB-IoT Technology," *Mob. Inf. Syst.*, 2021 (2021): 7801365:1-7801365:10.
- [4] R. D. Yates, Y. Sun, D. R. Brown, S. K. Kaul, E. Modiano and S. Ulukus, "Age of Information: An Introduction and Survey," *IEEE Journal on Selected Areas in Communications*, vol. 39, no. 5, pp. 1183-1210, 2021.
- [5] Yin Sun; Igor Kadota; Rajat Talak; Eytan Modiano, *Age of Information: A New Metric for Information Freshness*, Morgan & Claypool, 2019.
- [6] M. A. Abd-Elmagid, N. Pappas and H. S. Dhillon, "On the Role of Age of Information in the Internet of Things," *IEEE Communications Magazine*, vol. 57, no. 12, pp. 72-77, December 2019.
- [7] Antzela Kosta; Nikolaos Pappas; Vangelis Angelakis, *Age of Information: A New Concept, Metric, and Tool*, Now Press, 2017.
- [8] S. Kaul, M. Gruteser, V. Rai, and J. Kenney, Minimizing age of information in vehicular networks, *Proc. 8th Annual IEEE Commun. Soc. Conf. Sensor, Mesh Ad Hoc Commun. Netw.*, pp. 350-358, 2011.
- [9] S. Kaul, R. Yates, and M. Gruteser, Real-time status: How often should one update? *Proc. IEEE Int. Conf. Comput. Commun. (INFOCOM)*, Orlando, FL, 2012, pp. 2731-2735.
- [10] D. Qiao and M. C. Gursoy, "Age Minimization for Status Update Systems with Packet Based Transmissions over Fading Channels," *2019 11th International Conference on Wireless Communications and Signal Processing (WCSP)*, Xi'an, China, 2019, pp. 1-6.
- [11] B. Zhou and W. Saad, "Optimal Sampling and Updating for Minimizing Age of Information in the Internet of Things," *2018 IEEE Global Communications Conference (GLOBECOM)*, Abu Dhabi, United Arab Emirates, 2018, pp. 1-6.
- [12] J. Wang, T. Cao, X. Wang, M. Zhang and J. Guan, "Resource Scheduling in Vehicular Networks with Age of Information and Channel Awareness," *2022 IEEE/CIC International Conference on Communications in China (ICCC)*, Sanshui, Foshan, China, 2022, pp. 344-349.
- [13] B. Wang, S. Feng and J. Yang, "When to preempt? Age of information minimization under link capacity constraint," *Journal of Communications and Networks*, vol. 21, no. 3, pp. 220-232, June 2019.
- [14] N. Akar and O. Dogan, "Discrete-Time Queueing Model of Age of Information With Multiple Information Sources," *IEEE Internet of Things Journal*, vol. 8, no. 19, pp. 14531-14542, 1 Oct.1, 2021.
- [15] L. Liu, H. H. Yang, C. Xu and F. Jiang, "On the Peak Age of Information in NOMA IoT Networks With Stochastic Arrivals," *IEEE Wireless Communications Letters*, vol. 10, no. 12, pp. 2757-2761, Dec. 2021.
- [16] I. Kadota and E. Modiano, "Age of Information in Random Access Networks with Stochastic Arrivals," *IEEE INFOCOM 2021 - IEEE Conference on Computer Communications*, 2021, pp. 1-10.
- [17] I. Kadota and E. Modiano, "Minimizing the Age of Information in Wireless Networks with Stochastic Arrivals," *IEEE Transactions on Mobile Computing*, vol. 20, no. 3, pp. 1173-1185, 2021.
- [18] I. Kadota, A. Sinha and E. Modiano, "Optimizing Age of Information in Wireless Networks with Throughput Constraints," *IEEE INFOCOM 2018 - IEEE Conference on Computer Communications*, 2018, pp. 1844-1852.
- [19] I. Kadota, A. Sinha, E. Uysal-Biyikoglu, R. Singh and E. Modiano, "Scheduling Policies for Minimizing Age of Information in Broadcast Wireless Networks," *IEEE/ACM Transactions on Networking*, vol. 26, no. 6, pp. 2637-2650, 2018.
- [20] C. Li, S. Li, Y. Chen, Y. Thomas Hou and W. Lou, "AoI Scheduling with Maximum Thresholds," *IEEE INFOCOM 2020 - IEEE Conference on Computer Communications*, 2020, pp. 436-445.
- [21] R. V. Bhat, R. Vaze and M. Motani, "Age of Information Minimization in Fading Multiple Access Channels," *IEEE INFOCOM 2020 - IEEE Conference on Computer Communications Workshops (INFOCOM WKSHPS)*, 2020, pp. 948-953.
- [22] M. Moltafet, M. Leinonen and M. Codreanu, "On the Age of Information in Multi-Source Queueing Models," *IEEE Transactions on Communications*, vol. 68, no. 8, pp. 5003-5017, 2020.
- [23] J. Chen et al., "On the Adaptive AoI-aware Buffer-aided Transmission Scheme for NOMA Networks," *2021 IEEE Wireless Communications and Networking Conference (WCNC)*, 2021, pp. 1-6.
- [24] J. Sun, L. Wang, Z. Jiang, S. Zhou and Z. Niu, "Age-Optimal Scheduling for Heterogeneous Traffic With Timely Throughput Constraints," *IEEE Journal on Selected Areas in Communications*, vol. 39, no. 5, pp. 1485-1498, 2021.
- [25] N. Hirotsawa, H. Iimori, K. Ishibashi and G. T. F. D. Abreu, "Minimizing Age of Information in Energy Harvesting Wireless Sensor Networks," *IEEE Access*, vol. 8, pp. 219934-219945, 2020.
- [26] R. Zhang and C. K. Ho, "MIMO Broadcasting for Simultaneous Wireless Information and Power Transfer," *IEEE Transactions on Wireless Communications*, vol. 12, no. 5, pp. 1989-2001, 2013.
- [27] Q. Shi, L. Liu, W. Xu and R. Zhang, "Joint Transmit Beamforming and Receive Power Splitting for MISO SWIPT Systems," *IEEE Transactions on Wireless Communications*, vol. 13, no. 6, pp. 3269-3280, 2014.
- [28] E. Boshkovska, D. W. K. Ng, N. Zlatanov and R. Schober, "Practical Non-Linear Energy Harvesting Model and Resource Allocation for SWIPT Systems," *IEEE Communications Letters*, vol. 19, no. 12, pp. 2082-2085, 2015.
- [29] H. Ju and R. Zhang, "Optimal resource allocation in full-duplex wireless-powered communication network," *IEEE Transactions on Communications*, vol. 62, no. 10, pp. 3528-3540, 2014.
- [30] X. Lu, P. Wang, D. Niyato, D. I. Kim and Z. Han, "Wireless Networks With RF Energy Harvesting: A Contemporary Survey," *IEEE Communications Surveys & Tutorials*, vol. 17, no. 2, pp. 757-789, 2015.
- [31] X. Chen, X. Wang and X. Chen, "Energy-Efficient Optimization for Wireless Information and Power Transfer in Large-Scale MIMO Sys-

- tems Employing Energy Beamforming," *IEEE Wireless Communications Letters*, vol. 2, no. 6, pp. 667-670, 2013.
- [32] Q. Sun, G. Zhu, C. Shen, X. Li and Z. Zhong, "Joint Beamforming Design and Time Allocation for Wireless Powered Communication Networks," *IEEE Communications Letters*, vol. 18, no. 10, pp. 1783-1786, 2014.
- [33] M. M. Razlighi and N. Zlatanov, "Buffer-aided relaying for the two-hop full-duplex relay channel with self-interference," *IEEE Transactions on Wireless Communications*, vol. 17, no. 1, pp. 477-491, Jan. 2018.
- [34] F. L. Duarte and R. C. de Lamare, "Buffer-Aided Max-Link Relay Selection for Multi-Way Cooperative Multi-Antenna Systems," *IEEE Communications Letters*, vol. 23, no. 8, pp. 1423-1426, Aug. 2019.
- [35] J. Gu, R. C. de Lamare and M. Huemer, "Buffer-Aided Physical-Layer Network Coding With Optimal Linear Code Designs for Cooperative Networks," *IEEE Transactions on Communications*, vol. 66, no. 6, pp. 2560-2575, June 2018.
- [36] Y. Gong, G. Chen and T. Xie, "Using Buffers in Trust-Aware Relay Selection Networks With Spatially Random Relays," *IEEE Transactions on Wireless Communications*, vol. 17, no. 9, pp. 5818-5826, Sept. 2018.
- [37] K. W. Choi and D. I. Kim, "Stochastic Optimal Control for Wireless Powered Communication Networks," *IEEE Transactions on Wireless Communications*, vol. 15, no. 1, pp. 686-698, Jan. 2016.
- [38] X. Lan, Q. Chen and L. Cai, "Wireless Powered Buffer-Aided Communication Over K -User Interference Channel," *2018 IEEE 88th Vehicular Technology Conference (VTC-Fall)*, 2018, pp. 1-6.
- [39] Y. Liu, Q. Chen and X. Tang, "Adaptive Buffer-Aided Wireless Powered Relay Communication With Energy Storage," *IEEE Transactions on Green Communications and Networking*, vol. 2, no. 2, pp. 432-445, 2018.
- [40] X. Lan, Q. Chen, L. Cai and L. Fan, "Buffer-Aided Adaptive Wireless Powered Communication Network With Finite Energy Storage and Data Buffer," *IEEE Transactions on Wireless Communications*, vol. 18, no. 12, pp. 5764-5779, 2019.
- [41] M. A. Abd-Elmagid, H. S. Dhillon and N. Pappas, "A Reinforcement Learning Framework for Optimizing Age of Information in RF-Powered Communication Systems," *IEEE Transactions on Communications*, vol. 68, no. 8, pp. 4747-4760, Aug. 2020.
- [42] Q. Zhou, C. Tan, H. Li, J. Bian, H. Liu and M. Zheng, "Periodic Data Scheduling Scheme for Power Internet of Things Based on Age of Information," *2023 IEEE 97th Vehicular Technology Conference (VTC2023-Spring)*, Florence, Italy, 2023.
- [43] Y. Ji and X. Xu, "Single Threshold Packet Scheduling Policy for AoI Minimization in Resource-Constrained Network," *2022 14th International Conference on Wireless Communications and Signal Processing (WCSP)*, Nanjing, China, pp. 990-995, 2022.
- [44] M. A. Abd-Elmagid, H. S. Dhillon and N. Pappas, "AoI-Optimal Joint Sampling and Updating for Wireless Powered Communication Systems," *IEEE Transactions on Vehicular Technology*, vol. 69, no. 11, pp. 14110-14115, Nov. 2020.
- [45] N. Lu, B. Ji, and B. Li, "Age-based Scheduling: Improving Data Freshness for Wireless Real-Time Traffic," *Mobihoc'18: Proceedings of the Eighteenth ACM International Symposium on Mobile Ad Hoc Networking and Computing*, pp.191-200, June 2018.
- [46] I. Kadota, A. Sinha and E. Modiano, "Scheduling Algorithms for Optimizing Age of Information in Wireless Networks With Throughput Constraints," *IEEE/ACM Transactions on Networking*, vol. 27, no. 4, pp. 1359-1372, Aug. 2019.
- [47] M. J. Neely, "Stochastic Network Optimization with Application to Communication and Queuing Systems," *Synthesis Lectures on Communication Networks*, vol. 3, no. 1, pp. 1-211, 2010.